Chemical Science

ROYAL SOCIETY OF CHEMISTRY

EDGE ARTICLE

View Article Online
View Journal | View Issue

Cite this: *Chem. Sci.*, 2021, **12**, 5171

All publication charges for this article have been paid for by the Royal Society of Chemistry

Received 15th January 2021
Accepted 23rd February 2021

DOI: 10.1039/d1sc00272d

rsc.li/chemical-science

Hybridized local and charge-transfer excited state fluorophores enabling organic light-emitting diodes with record high efficiencies close to 20%†

Tiantian Liu,[a] Xiaojie Chen,[a] Juan Zhao,[*b] Weichun Wei,[a] Zhu Mao,[*c] William Wu,[d] Shibo Jiao,[d] Yang Liu,[d] Zhiyong Yang[a] and Zhenguo Chi[*ab]

Pure organic emitters with full utilization of triplet excitons are in high demand for organic light-emitting diodes (OLEDs). Herein, through modulation of electron donors and introduction of phenyl rings as π spacers, we present three pure organic fluorophores (BCz, BTCz and BPTCz) with the hybridized local and charge-transfer (HLCT) excited state feature for OLED fabrication. Importantly, the introduction of π spacers in BPTCz not only enhances locally excited character with a fast radiative decay but also promotes intermolecular interactions to suppress non-radiative decays, contributing to a high solid-state fluorescence efficiency over 90%. Significantly, BPTCz not only endows its doped OLEDs with an external quantum efficiency (EQE) up to 19.5%, but also its non-doped OLED with a high EQE of 17.8%, and these outstanding efficiencies are the state-of-the-art performances of HLCT-based OLEDs.

Introduction

The exploration of high-efficiency organic emitters has drawn much attention due to their crucial applications in organic light-emitting diodes (OLEDs) since the first work reported by Tang and co-authors.[1] In OLEDs, the recombination of holes and electrons can form singlet and triplet excitons in a ratio of 1 : 3 according to spin statistics.[2] However, approximately 75% triplet excitons decay through non-radiative processes because of the spin-forbidden transition between the singlet and triplet, leading to the limitation of the external quantum efficiency (EQE) to 5% in conventional fluorescent devices. Therefore, the effective utilization of triplet excitons in organic emitters is very essential for constructing high-efficiency OLEDs. Recent efforts have paved a way to utilize the triplet excitons in thermally activated delayed fluorescent (TADF) molecules,[3,4] which possess a narrow singlet–triplet energy splitting (ΔE_{ST}) because of the charge transfer (^{1}CT) feature. The up-conversion with a spin-flip process of the lowest dark triplet (T_1) to the lowest emissive singlet state (S_1) is activated *via* thermally assisted reverse intersystem crossing (RISC), leading to a maximal EQE with a breakthrough of the spin statistical limitation. Nevertheless, the first-order coupling between ^{1}CT singlet and ^{3}CT triplet is inefficient in TADF molecules[5] (Fig. 1a), which results in slow up-conversion and thereby efficiency roll-off in TADF-based OLEDs. In contrast, the coupling between ^{1}CT and the locally excited-state (^{3}LE) is much more effective due to the large spin–orbit coupling (SOC). Consequently, the second-order coupling with an intermediate state (^{3}LE) is introduced to

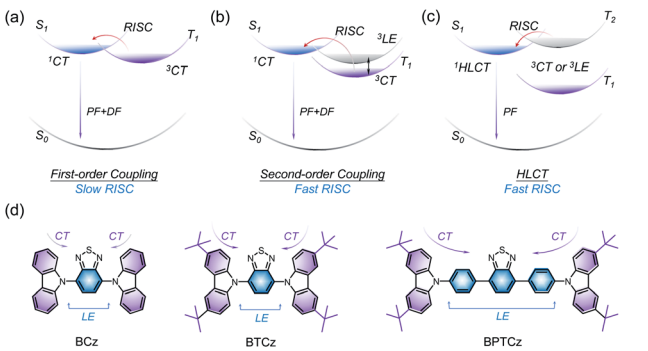

Fig. 1 Proposed mechanism of (a) first-order coupling in TADF molecules, (b) second-order coupling in TADF molecules, (c) HLCT molecules and (d) molecular structures of the HLCT emitters presented in this work. PF: prompt fluorescence, DF: delayed fluorescence.

[a]*PCFM Lab, GDHPPC Lab, Guangdong Engineering Technology, Research Center for High-performance Organic and Polymer Photoelectric Functional Films, State Key Laboratory of OEMT, School of Chemistry, Sun Yat-sen University, Guangzhou 510275, China. E-mail: chizhg@mail.sysu.edu.cn*

[b]*State Key Laboratory of OEMT, School of Materials Science and Engineering, Sun Yat-sen University, Guangzhou 510275, China. E-mail: zhaoj95@mail.sysu.edu.cn*

[c]*Shenzhen Institute of Advanced Electronic Materials, Shenzhen Institutes of Advanced Technology, Chinese Academy of Sciences, Shenzhen 518055, China. E-mail: maozhu3@mail.sysu.edu.cn*

[d]*R&D Center, Shenzhen China Star Optoelectronics Semiconductor Display Technology Co., Ltd, Shenzhen 518132, China*

† Electronic supplementary information (ESI) available. CCDC 2021326, 2021331 and 2021355. For ESI and crystallographic data in CIF or other electronic format see DOI: 10.1039/d1sc00272d

achieve fast RISC rates in TADF molecules (Fig. 1b) which contain multiple donor (D) and acceptor (A) moieties.[6]

In order to take full advantages of LE and CT excitons, Ma and colleagues have established a distinctive type of organic emitters in which the lowest singlet state exhibits a hybridized local and charge-transfer (HLCT) feature.[7] In this excited system, the RISC process occurs at upper excited states *via* a "hot exciton" channel (Fig. 1c). Due to the strong coupling between the ^{1}HLCT state and ^{3}LE or ^{3}CT, the RISC is promoted with a very fast rate which avoids long-lived components and thus benefits the reduction of efficiency roll-off in OLEDs. Additionally, the radiative rate of the HLCT state is much higher than the radiative rate of ^{1}CT in TADF molecules, allowing the radiative process to compete with non-radiative pathways in the first place. The typical HLCT molecules are composed of D and A segments and thus the well-regulated dihedral angles of D–A can modulate the character of excited states and energy-level arrangement to promote the radiative decays and RISC process. Therefore, the performance of HLCT molecules greatly depends on the ability of donors, acceptors, and π spacers. In order to enable high-performance OLEDs, the building blocks of HLCT emitters should be carefully selected to regulate appropriate electron push–pull strength.

Here, we report three D–(π)–A emitters, namely BCz, BTCz, and BPTCz (Fig. 1d), which are based on a combination of benzothiadiazole and carbazole derivative groups. The relationship between the molecular structure and HLCT excited-state character is well understood through UV-Vis absorption, photoluminescence (PL), transient spectra, and theoretical simulations. Importantly, the influence of π spacers between D and A moieties is also studied, which plays a pivotal role in HLCT emitters. BPTCz with π spacers exhibits fairly efficient RISC of "hot exciton", due to the large oscillator strength between S_1 and S_0 (efficient radiation), narrow energy split of T_2 and S_1 (fast RISC), and large gap between T_1 and T_2 (low interconversion). Therefore, BPTCz affords both doped and non-doped OLEDs with high EQEs close to 20%, which are the highest efficiencies of HLCT-based OLEDs reported so far.

Results and discussion

Photophysical properties

The synthetic routes for BCz, BTCz and BPTCz are shown in Scheme S1,† and meanwhile the three compounds possess excellent thermal properties (Fig. S13 and Table S1†) that are favorable for OLED applications. The UV-Vis absorption spectra and PL spectra of BCz, BTCz and BPTCz films are displayed in Fig. 2a. The main absorption peak is located at 463, 477 and 430 nm for BCz, BTCz and BPTCz, respectively. In comparison with the PL spectrum of BCz with a PL peak (λ_{max}) of 590 nm, when the *tert*-butyl groups are introduced into the donor unit, the resulting BTCz demonstrates a spectral red-shift ($\lambda_{max} = 614$ nm), due to the enhanced donating ability of the *tert*-butyl groups. However, BPTCz with phenyl bridges displays a spectral blue-shift ($\lambda_{max} = 564$ nm), in spite of enlarged conjugation. The same spectral shifts are also observed from their UV-Vis absorption and PL spectra in solution state (Fig. S14†). The

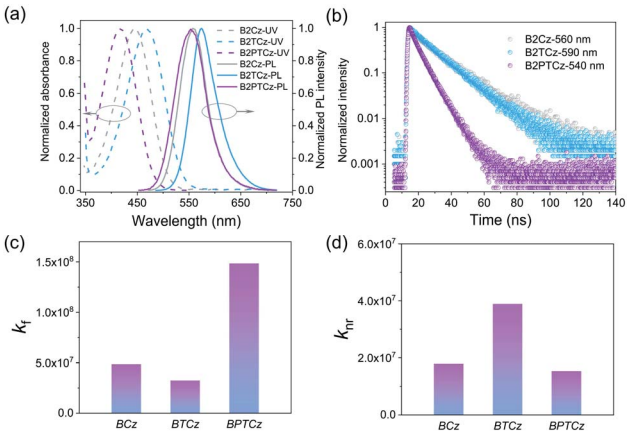

Fig. 2 (a) UV-Vis absorption and PL spectra, (b) transient PL decay curves, (c) radiative rates and (d) non-radiative rates for BCz, BTCz and BPTCz films.

variations of the UV-Vis absorption and PL spectra imply that the modifications of the donor moiety and π spacer can greatly affect the photophysical properties of organic emitters. Furthermore, the intramolecular charge transfer (ICT) feature of the three compounds can be verified by the bathochromic shifts of their PL spectra as the solvent polarity increases (Fig. S16†), along with considerably broadened full-wavelength at half-maximum.[8] As for the solid-state BCz, BTCz and BPTCz, their neat films exhibit a PL quantum yield (PLQY) of 73.0%, 45.5%, and 90.6%, respectively. To better understand the fluorescence behaviors of the three compounds, transient PL measurements were performed. As shown in Fig. 2b and S16–S18,† the BCz, BTCz and BPTCz neat films demonstrate a single exponential decay feature with a prompt lifetime of 15.0, 14.0, and 6.1 ns, respectively, which is related to the fluorescence emission from a sole excited state. Additionally, temperature-dependent transient decays were also performed. As shown in Fig. S17–S19 and Table S2,† the lifetimes of the emitters are hardly changed while the temperature varies. These results confirm the fluorescence feature of the excited states and thus exclude the TADF process in these molecules. Moreover, the blue shifted emission and shortened lifetime suggest an enhanced LE component of the lowest singlet state in BPTCz when compared with that of BCz and BTCz.[9] Additionally, the radiative decay rate constants (k_r) of fluorescence and non-radiative decay rate constants (k_{nr}) are estimated from the PLQY and lifetime (Fig. 2c and d). It is found that BPTCz with π spacers not only exhibits a much higher radiative rate than BCz and BTCz, but also a lower non-radiative decay rate, which are beneficial for achieving high-performance OLEDs.

Theoretical studies

In order to examine the excited states of BCz, BTCz and BPTCz, theoretical calculations were conducted by using the density functional theory (DFT) and time-dependent DFT (m062x/6-311g(d)). As plotted in Fig. S20,† the highest occupied molecular orbitals (HOMOs) of the three compounds are mostly

distributed on the whole molecules, the lowest unoccupied molecular orbitals (LUMOs) of BCz and BTCz are mainly located on the benzothiadiazole acceptor, while the LUMO of BPTCz is located on the benzothiadiazole core and also extended to the adjacent phenyl rings. Moreover, natural transition orbital (NTO) analyses were also performed to explore the excited states and transition characters in these D–(π)–A molecules (Fig. S21–S23†). As displayed in Fig. 3a, the S_1 of the three molecules present a hybrid feature of LE and CT, demonstrating their HLCT features of the excited-states. In BPTCz, the S_1 state exhibiting a stronger LE character can render faster radiation decay, as the LE state is more efficiently radiative than the CT state.[10] The much higher oscillator strength ($f = 0.8681$) of BPTCz is well consistent with the faster radiative decay through experiment ($k_r = 1.48 \times 10^8\ s^{-1}$). The NTO results demonstrate that the introduction of phenyl rings as π spacers can well modulate the excited state (S_1) with more LE component so as to enhance radiative decay and lead to a higher PLQY in BPTCz.

In a further set of experiments, the energy-level arrangements and spin–orbit coupling (SOC) matrix elements of the three molecules were studied. As illustrated in Fig. 3b, all the compounds exhibit very low energy levels of T_1 and large energy gaps between T_1 and T_2, which can suppress interconversion (IC) transition from T_2 to T_1. Importantly, a small energy difference between S_1 and T_2 is found for the three molecules, which triggers the spin-flip at higher-lying excited states, and thus results in a fast RISC process occurring from T_2 to S_1 (Fig. 3b) to avoid concentration quenching of triplet excitons.[11,12] In detail, BPTCz exhibits the narrowest energy difference between S_1 and T_2, implying that there is a higher possibility for the occurrence of the RISC process. Meanwhile, BPTCz with π spacers shows the largest energy difference between T_2 and T_1, suggesting great reduction of the IC rate. Consequently, the RISC process is more efficient to enable exciton distribution on S_1. It should be noted that all the molecules present a relatively high SOC constant ($\sim$0.5 cm^{-1}) between S_1 and T_2, which is likely associated with the various heteroatoms in the molecules.[13] With the help of the narrow gap and large SOC constant, the spin-flip between T_2 and S_1 is very efficient to take full utilization of the triplet excitons.

Generally, excited-molecular motions can be suppressed by intra- and intermolecular interactions to render a lower k_{nr}. Firstly, reduced density gradient (RDG) isosurface maps of the molecules were studied to investigate the intramolecular interactions.[14–16] As illustrated in Fig. 4a, relatively stronger intramolecular interactions are observed in BCz rather than BTCz and BPTCz. To gain further insights into conformation changes of ground state (S_0) and excited state (S_1) in the molecules, root-mean-square-deviation (RMSD) calculations were carried out to reflect the non-radiation behavior induced by conformation changes (Fig. 4b).[17] In the case of BCz, the conformation changes of S_0 and S_1 are mainly induced by the rotation of the carbazole moieties. As for BTCz with

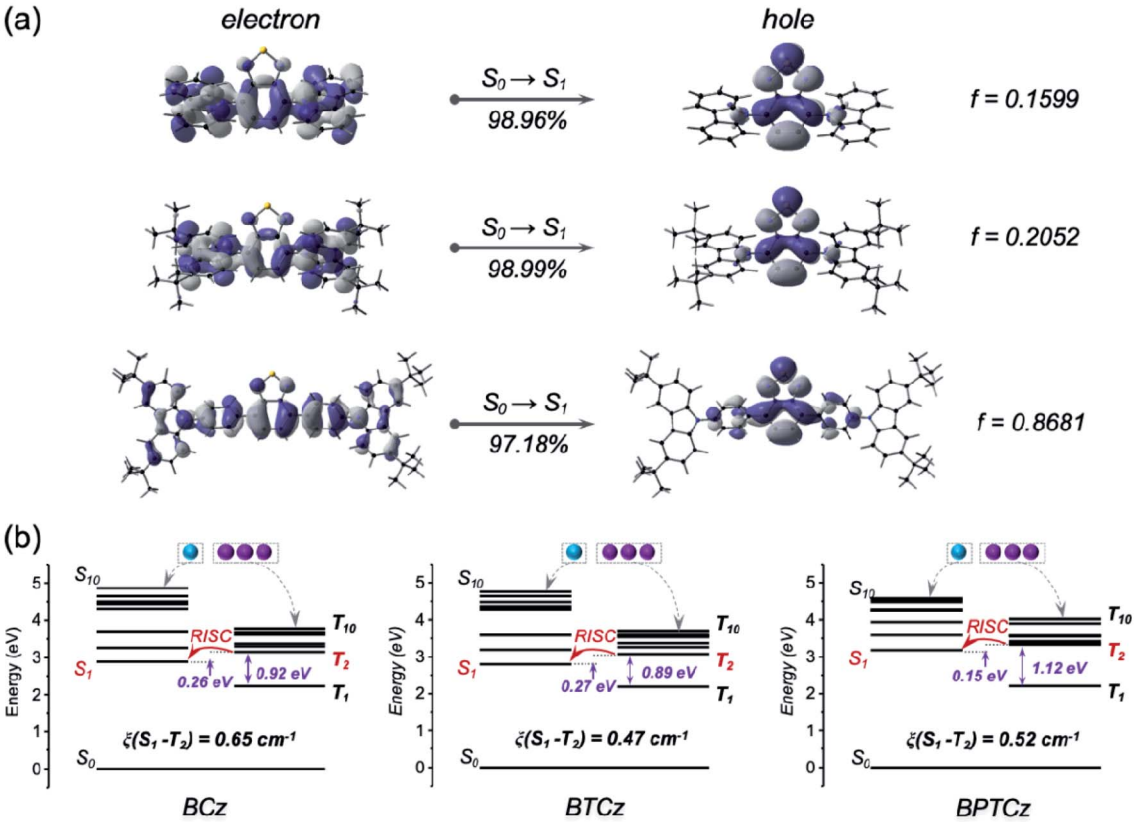

Fig. 3 (a) NTO distributions for the S_1 state and (b) energy level diagrams including SOC constants (ξ) of BCz, BTCz and BPTCz.

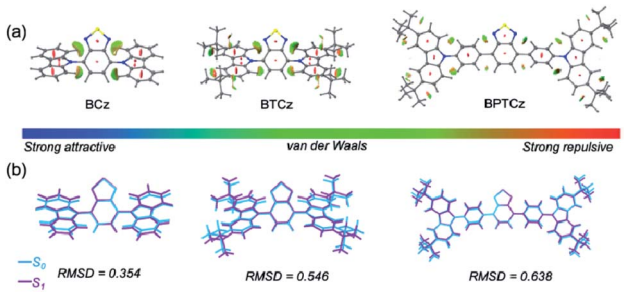

Fig. 4 (a) Geometries of S_0 and S_1, and (b) reduced density gradient isosurface maps of BCz, BTCz and BPTCz.

incorporation of *tert*-butyl units, the conformation changes are mainly contributed by the rotation of carbazole groups as well as the peripheral *tert*-butyl units. Accordingly, BTCz shows larger conformation changes than BCz. The higher RMSD values indicate the existence of more molecular motions that could induce faster non-radiative transitions ($k_{nr} = 1.80 \times 10^7$ s^{-1} for BCz and $k_{nr} = 3.89 \times 10^7$ s^{-1} for BTCz through experimental results), leading to a lower PLQY in BTCz. However, BPTCz has a large RMSD value of 0.636 but shows a higher PLQY (90.6%) and a lower k_{nr} (1.54×10^7 s^{-1}), which implies that there are some other factors affecting the emission behaviors of BPTCz rather than the intramolecular interactions, such as intermolecular interactions. In this light, the molecular packing in a single crystal was further examined to reconcile the conflict. As shown in Fig. S24,† BPTCz adopts a parallel arrangement as the π–π stacking mode in the crystal, and efficient D–A electrostatic interaction between adjacent molecules improves the intermolecular interaction (Fig. S25†), which can effectively restrict the molecular excited state vibration and suppress the non-radiative pathways. Meanwhile, the presence of steric hindrance of the *tert*-butyl groups prevents further molecular close-packing of adjacent D and A moieties, thereby inhibiting the notorious aggregation that causes quenching. In contrast, close π–π stacking ($d = 3.352$ Å) is formed in BCz due to the lack of *tert*-butyl groups (Fig. S26†). Nevertheless, the three compounds exhibit obvious intra- and inter-molecular interactions to suppress vibration motions of excited molecules, and thereby restrict non-radiative transitions. As a result, the molecules are endowed with high fluorescence efficiencies that are beneficial for constructing high-performance OLEDs, especially BPTCz with π spacers.

Device performance

Electroluminescence (EL) performances of the three compounds were further investigated. By a thermal evaporation approach, doped OLEDs with the device structure as: ITO/PEDOT:PSS (30 nm)/MCP (20 nm)/EML (28 nm)/TPBI (40 nm)/LiF (1 nm)/Al (100 nm) were fabricated, wherein *m*-bis(*N*-carbazolyl)benzene (MCP) and 1,3,5-tris(*N*-phenylbenzimidazol-2-yl)benzene (TPBI) work as the hole transporting layer and electron transporting layer, respectively. As for the EML, the emitters were doped into a common host (CBP) with a doping ratio of 40 wt%. The EL performances are summarized in Table 1 and displayed in Fig. 5. As seen from Fig. 5a, the doped BPTCz device achieves a maximal luminance of 33 190 cd m^{-2}, which is 18 150 and 7680 cd m^{-2} in the doped BCz and BTCz devices, respectively. Meanwhile, a maximal EQE of 9.3% and 7.3% is obtained in the doped BCz and BTCz devices, respectively. Impressively, a maximal EQE reaching up to 19.5% is realized in the doped BPTCz device (Fig. 5b). To our knowledge, such a high EQE is the highest efficiency of HLCT-mechanism based OLEDs (Table S3†),[18–20] which cover HLCT-based OLEDs showing different color emissions. Given that promising studies on HLCT just appeared a few years ago, high-efficiency HLCT emitters are still rare; notably, this work is the first example to realize high EQEs close to 20% in HLCT-based OLEDs. It is also worth mentioning that the high EQEs afforded by the BPTCz-based devices are even comparable to those of the best-performing TADF-based OLEDs.[4,21–23] These results confirm the practicability of HLCT materials as high-efficiency OLED emitters. Moreover, it is found that BCz, BTCz and BPTCz also endow their non-doped OLEDs with excellent device performances (Fig. S29†), given the fact that fast k_r and k_{RISC} of the emitters help to guarantee high efficiency in neat films. For instance, the non-doped BPTCz device exhibits a maximal EQE as high as 17.8%, while that of the non-doped BCz and BTCz devices is 9.1% and 7.4%, respectively. Therefore, with regard to BCz, BTCz and BPTCz, each compound enables its doped and non-doped OLEDs with comparable device performances,

Table 1 Device performance of the OLEDs

	EML	L_m[a] (cd m^{-2})	CE_m[b] (cd A^{-1})	PE_m[c] (lm W^{-1})	EQE_m[d] (%)	λ_{EL}[e] (nm)
Thermal evaporation	CBP:BCz	18 150	28.5	17.9	9.3	568
	CBP:BTCz	7680	14.4	7.5	7.3	598
	CBP:BPTCz	33 190	65.5	37.4	19.5	546
	BCz	15 590	23.4	14.7	9.1	583
	BTCz	10 960	14.8	9.3	7.4	600
	BPTCz	23 640	57.5	30.1	17.8	552
Solution processing	CBP:BCz	7740	8.4	5.3	2.7	566
	CBP:BTCz	7260	7.4	4.6	3.2	594
	CBP:BPTCz	14 980	20.5	10.0	6.0	546

[a] Max luminance. [b] Max current efficiency. [c] Max power efficiency. [d] Max EQE. [e] EL peak wavelength.

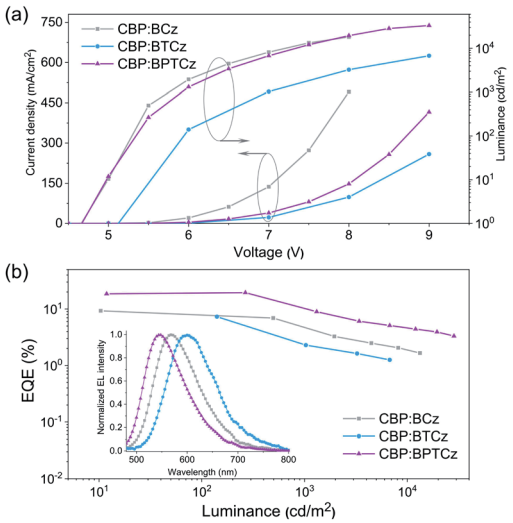

Fig. 5 (a) Current density–voltage–luminance curves and (b) EQE–luminance curves of doped OLEDs, inset: EL spectra.

although the doped OLEDs show slightly higher device performance, which is likely due to more effective suppression of exciton annihilations in the doped EML. In brief, these results verify that BCz, BTCz and BPTCz are attractive HLCT emitters allowing both doping and non-doping techniques to fabricate highly efficient OLEDs, especially BPTCz endowing high EQEs comparable to that of high-efficiency TADF emitters.

The steric hindrance of *tert*-butyl groups in molecules can help to enhance molecular solubility and decrease self-quenching of aggregated excitons in neat films by restricting excited-molecular motions and π–π stacking.[24] Therefore, solution-processed OLEDs based on BCz, BTCz, and BPTCz were also fabricated to evaluate their solution-processability. As displayed in Fig. S30,† the solution-processed BPTCz device achieves a maximal EQE of 6.0%, which is rarely reported in solution-processed OLEDs based on HLCT emitters (Table S4†).[25,26] With further optimization of device structure such as exploiting appropriate hole transporting materials and host materials, performance enhancement can be expected.

Conclusions

In summary, three pure organic HLCT emitters (BCz, BTCz and BPTCz) were systematically studied through structural modulation to take full utilization of triplet excitons. It was found that, on one hand, the phenyl rings acting as π bridges in BPTCz brought about more LE character and a higher radiative rate; on the other hand, the *tert*-butyl units in BPTCz contributed to enhanced intermolecular interactions and suppressed non-radiative decays. As a result, BPTCz neat film exhibited a much higher PLQY (90.6%) than BCz and BTCz. Remarkably, BPTCz enabled its non-doped and doped OLEDs with an impressive maximal EQE of 19.5% and 17.8%, respectively, which are the highest efficiencies of HLCT-mechanism based OLEDs reported so far. The excellent device performances confirm the effectiveness of our design strategy, and also the great potential of HLCT materials as pure organic high-efficiency emitters similar to the well-known TADF emitters for OLED applications.

Author contributions

T. Liu, Z. Mao, and J. Zhao designed the experiments. T. Liu performed the experiments with the help of X. Chen and W. Wei. Z. Mao carried out the theoretical calculations. All the authors were involved in the analysis and interpretation of the data. T. Liu, J. Zhao and Z. Mao wrote the manuscript. Z. Chi revised the manuscript. The financial supports for this work are mainly acquired by Z. Chi, J. Zhao, Z. Mao, and Shenzhen China Star Optoelectronics Semiconductor Display Technology Co., Ltd.

Conflicts of interest

There are no conflicts to declare.

Acknowledgements

This work was financially supported by the National Natural Science Foundation of China (NSFC: 51803242, 51733010, 51973239, 52073316, and 51603232), Science and Technology Planning Project of Guangdong (2015B090913003 and 2015B090915003), and Guangdong Natural Science Funds for Distinguished Young Scholar (2017B030306012).

Notes and references

1 C. W. Tang and S. A. VanSlyke, *Appl. Phys. Lett.*, 1987, **51**, 913–915.
2 M. Baldo, D. O'brien, M. Thompson and S. Forrest, *Phys. Rev. B: Condens. Matter Mater. Phys.*, 1999, **60**, 14422.
3 H. Uoyama, K. Goush, K. Shizu, H. Nomura and C. Adachi, *Nature*, 2012, **492**, 234–238.
4 Z. Yang, Z. Mao, Z. Xie, Y. Zhang, S. Liu, J. Zhao, J. Xu, Z. Chi and M. P. Aldred, *Chem. Soc. Rev.*, 2017, **46**, 915–1016.
5 M. K. Etherington, J. Gibson, H. F. Higginbotham, T. J. Penfold and A. P. Monkman, *Nat. Commun.*, 2016, **7**, 13680.
6 Z. Yang, Z. Mao, C. Xu, X. Chen, J. Zhao, Z. Yang, Y. Zhang, W. Wu, S. Jiao, Y. Liu, M. P. Aldred and Z. G. Chi, *Chem. Sci.*, 2019, **10**, 8129–8134.
7 Y. Pan, J. Huang, W. Li, Y. Gao, Z. Wang, D. Yu, B. Yang and Y. Ma, *RSC Adv.*, 2017, **7**, 19576–19583.
8 Z. Yang, E. Ubba, Q. Huang, Z. Mao, W. Li, J. Chen, J. Zhao, Y. Zhang and Z. Chi, *J. Mater. Chem. C*, 2020, **8**, 7384–7392.
9 S. Zhang, L. Yao, Q. Peng, W. Li, Y. Pan, R. Xiao, Y. Gao, C. Gu, Z. Wang, P. Lu, F. Li, S. Su, B. Yang and Y. Ma, *Adv. Funct. Mater.*, 2015, **25**, 1755–1762.
10 W. Li, Y. Pan, R. Xiao, Q. Peng, S. Zhang, D. Ma, F. Li, F. Shen, Y. Wang, B. Yang and Y. Ma, *Adv. Funct. Mater.*, 2014, **24**, 1609–1614.
11 W. Li, Y. Pan, L. Yao, H. Liu, S. Zhang, C. Wang, F. Shen, P. Lu, B. Yang and Y. Ma, *Adv. Opt. Mater.*, 2014, **2**, 892–901.

12 J. Yang, Q. Guo, J. Wang, Z. Ren, J. Chen, Q. Peng, D. Ma and Z. Li, *Adv. Opt. Mater.*, 2018, **6**, 1800342.
13 S. Cai, H. Shi, D. Tian, H. Ma, Z. Cheng, Q. Wu, M. Gu, L. Huang, Z. An, Q. Peng and W. Huang, *Adv. Funct. Mater.*, 2018, **28**, 1705045.
14 T. Lu and F. W. Chen, *J. Comput. Chem.*, 2012, **33**, 580–592.
15 J. E. Adams, W. W. Mantulin and J. R. Huber, *J. Am. Chem. Soc.*, 1973, **95**, 5477–5481.
16 H. Liu, Y. Gao, J. Cao, T. Li, Y. Wen, Y. Ge, L. Zhang, G. Pan, T. Zhou and B. Yang, *Mater. Chem. Front.*, 2018, **2**, 1853–1858.
17 W. Wei, Z. Yang, X. Chen, T. Liu, Z. Mao, J. Zhao and Z. Chi, *J. Mater. Chem. C*, 2020, **8**, 3663–3668.
18 X. Chen, Z. Yang, W. Li, Z. Mao, J. Zhao, Y. Zhang, Y.-C. Wu, S. Jiao, Y. Liu and Z. Chi, *ACS Appl. Mater. Interfaces*, 2019, **11**, 39026–39034.
19 J. Fan, Y. Zhang, K. Zhang, J. Liu, G. Jiang, F. Li, L. Lin and C.-K. Wang, *J. Mater. Chem. C*, 2019, **7**, 8874–8887.
20 T. Liu, L. Zhu, C. Zhong, G. Xie, S. Gong, J. Fang, D. Ma and C. Yang, *Adv. Funct. Mater.*, 2017, **27**, 1606384.
21 Y. Wang, Y. Zhang, K. Tong, L. Ding, J. Fan and L. S. Liao, *J. Mater. Chem. C*, 2019, **7**, 15301–15307.
22 L. Zhan, Y. Xiang, Z. Chen, K. Wu, S. Gong, G. Xie and C. Yang, *J. Mater. Chem. C*, 2019, **7**, 13953–13959.
23 J. Liang, C. Li, Y. Cui, Z. Li, J. Wang and Y. Wang, *J. Mater. Chem. C*, 2020, **8**, 1614–1622.
24 F. Xie, Z. An, M. Xie, Y. Li, G. Zhang, S. Zou, L. Chen, J. Chen, T. Cheng and J. Tang, *J. Mater. Chem. C*, 2020, **8**, 5769–5776.
25 H. Usta, D. Alimli, R. Ozdemir, E. Tekin, F. Alkan, R. Kacar, A. G. Altas, S. Dabak, A. G. Gürek, E. Mutlugun, A. F. Yazici and A. Can, *J. Mater. Chem. C*, 2020, **8**, 8047–8060.
26 H. Usta, D. Alimli, R. Ozdemir, S. Dabak, Y. Zorlu, F. Alkan, E. Tekin and A. Can, *ACS Appl. Mater. Interfaces*, 2019, **11**, 44474–44486.